Up-Conversion Luminescence and Temperature Characteristics Study of Ho^{3+}/Yb^{3+} Co-doped $NaGd(MoO_4)_2$ Phosphors

L. Wang, S.Y. Liu*, W.B. Song, Y.Y. Chang, J.X. Liu, Y.B. Wen and Q.M. Yu

School of Intelligence and Electronic Engineering, Dalian Neusoft University of Information, 0008 Lingshui Street, 116000 Dalian, China

Received: 20.04.2023 & Accepted: 12.06.2023

Doi: 10.12693/APhysPolA.144.87 *e-mail: liushengyi@neusoft.edu.cn

In order to obtain the maximum up-conversion luminescence intensity of Ho^{3+}/Yb^{3+}-doped $NaGd(MoO_4)_2$ phosphors, samples with $1.00\%Ho^{3+}/22.89\%Yb^{3+}$ doping concentration were prepared by high-temperature solid-phase method. The doping concentration of $1.00\%Ho^{3+}/22.89\%Yb^{3+}$ corresponds to the maximum luminescence intensity of red light excited by a 980 nm laser. X-ray diffraction analysis showed that the prepared samples were in pure $NaGd(MoO_4)_2$ phase. Under the excitation of a 980 nm laser, the measured and theoretical luminescence intensities of the optimal sample are close to each other. The relationship between different pumping currents and up-conversion luminescence intensity was tested. The red light of the sample was proved to be a two-photon process. Up-conversion luminescence mechanism of the sample was discussed in detail. Finally, we measured the emission spectrum of the optimal sample in the up-conversion to temperature. It was fitted using the fluorescence intensity ratio formula, and its relative sensitivity was calculated to be 0.0204 K^{-1} at 440 K.

topics: $NaGd(MoO_4)_2$ phosphor, two-photon process, temperature characteristic, up-conversion luminescence

1. Introduction

Rare earth ion-doped up-conversion luminescent materials have been a research hotspot in the field of luminescence [1–3]. Up-conversion luminescence uses the anti-Stokes principle, which is a phenomenon where the emission wavelength is less than the excitation wavelength. This kind of luminescent material has been widely used in imaging and medicine, especially in the field of temperature measurement [4–8], which has been favored by researchers in recent years. Rare earth up-conversion luminescence is stimulated mainly by near-infrared light (such as 808, 980, 1540 nm) to obtain anti-Stoke luminescence in the visible or ultraviolet region. Rare earth up-conversion luminescence originates from a specific $4f \rightarrow 4f$ shell transition and has the advantages of stable photochemistry, narrow luminescence band, and large anti-Stokes shift. Most of the up-conversion doping ion combinations at 980 nm are Yb^{3+}/Er^{3+}, Yb^{3+}/Tm^{3+}, Yb^{3+}/Ho^{3+}, and fluoride (such as $NaYF_4$) [9, 10] is the most preferred matrix material. Yb^{3+} ions have strong absorption at 980 nm, which can transfer energy to Er^{3+} ions to improve the luminescence efficiency. Fluoride matrix materials have low phonon energy, which can effectively suppress the non-radiative energy loss of the excited state, thereby improving the luminescence efficiency [11]. However, the ionicity of fluoride materials leads to their unstable chemical properties, which limits their application to some extent. It is interesting to note that some oxide up-conversion luminescent materials with higher phonon energy in the matrix, such as $RE_2(MO_4)_3{:}Ln^{3+}$, $REVO_4{:}Ln^{3+}$, $NaRE(WO_4)_2{:}Ln^{3+}$, also have strong up-conversion luminescent properties [12–16]. In fact, in the up-conversion luminescence process, appropriate phonon assistance can bring new up-conversion population channels, which can improve the up-conversion luminescence properties of oxide matrix materials. In addition to doping ions, the selection of matrix materials is one of the important factors that determine the performance. Molybdate has always been an excellent matrix material. This material has excellent stability and good luminescent properties. $NaGd(MoO_4)_2$ is a kind of molybdate, but it has been rarely studied as a matrix material. However, as an important luminescent material, molybdate has important applications in many fields. In molybdate with $ARe(MoO_4)_2$ (A is an alkali metal element, Re is a rare earth element) chemical formula, the molybdenum ion is surrounded by four O^{2-} ions, located in the

tetrahedron center of symmetry, so $(MoO_4)^{2-}$ has good stability. Molybdate has a wide and strong charge transfer band in the near ultraviolet region, which can effectively absorb blue-violet light energy and transfer to doped rare earth ions. Therefore, molybdate is considered a promising phosphor material.

In order to obtain the maximum red up-conversion luminescence intensity of Ho^{3+}/Yb^{3+} co-doped $NaGd(MoO_4)_2$ phosphors, Ho^{3+}/Yb^{3+} doping and $NaGd(MoO_4)_2$ phosphors were prepared by high-temperature solid-phase method. After obtaining Ho^{3+}/Yb^{3+}-doped samples prepared by high-temperature solid-phase method, spectra of Ho^{3+}/Yb^{3+}-doped $NaGd(MoO_4)_2$ phosphors excited at 980 nm were studied in detail. Up-conversion luminescence spectra of Ho^{3+}/Yb^{3+}-doped $NaGd(MoO_4)_2$ phosphors excited at 980 nm are discussed. In addition, the activation energy of temperature quenching for the sample is calculated.

2. Experiment

2.1. Sample preparation

There are many ways to prepare phosphors. In this paper, the high-temperature solid-state method was used to prepare phosphors for up-conversion luminescence. First, the stoichiometric molar ratio of each reagent from the chemical molecular formula of the target product and the concentration of diluted ions are calculated. The mass of each reagent should be accurately calculated according to the molar ratio, and then each raw material and auxiliary drug solvent should be accurately weighted using an electronic balance. Raw materials include Na_2CO_3 (AR), Gd_2O_3 (AR), MoO_3 (AR), Ho_2O_3 (AR), Yb_2O_3 (AR). The weighed pharmaceutical ingredients are placed in a mortar and ground for 30 min until all reagents are evenly mixed. Then, the ground powder sample is loaded into a corundum crucible and calcined in a muffle furnace at 1050° for 4 h. The sample is naturally cooled to room temperature and taken out. Finally, the obtained bulk sample is placed in a mortar, ground, and then collected in a collection tube. All samples from the same group must be weighed simultaneously, crushed with the same force, and baked simultaneously in the same muffle furnace to ensure that the data obtained are comparable and the results are reliable, as only the ion permeation concentration is different in the same group of samples.

In order to obtain the maximum up-conversion luminescence intensity of Ho^{3+}/Yb^{3+}-doped $NaGd(MoO_4)_2$ phosphors, the Ho^{3+}/Yb^{3+} doping concentration range was initially optimized using a uniform design method. The binary quadratic regression equation of Ho^{3+}/Yb^{3+} doping concentration and maximum luminescence intensity was established by the general design of the quadratic rotation combination. Finally, the optimal solution of the regression equation was solved by genetic algorithm, i.e., the doping concentration of $1\%Ho^{3+}/22.89\%Yb^{3+}$ corresponds to the maximum luminescence intensity of red light excited by 980 nm laser.

2.2. Sample testing

In this paper, X-ray diffractometer (XRD-6000), F-4600 fluorescence spectrometer, 980 nm infrared laser, and DMU-450 automatic temperature control system are mainly used to characterize and analyze the crystal structure, optical properties, and performance of the samples. The phase structure and crystal structure of the prepared samples were analyzed using an X-ray powder diffractometer from Shimadzu Corporation (Model XRD-6000) in Japan. The instrument uses a Cu target (K radiation $\lambda = 0.15406$ nm) with an acceleration voltage of 40 kV and a working current of 30 mA. Using a fluorescence spectrometer manufactured by Hitachi (Hitachi, F-4600), the excitation spectrum, emission spectrum, and fluorescence attenuation curve of the prepared sample were measured, with a test wavelength range of 200–900 nm. The excitation source is a 980 nm fiber laser produced by Beijing Kaiprin Company. The maximum output power of the 980 nm laser is 2 W. At the same time, a proprietary temperature controller is used to heat the sample, thereby controlling the real-time temperature of the sample during the spectral characterization process.

3. Results and discussions

3.1. Preparation of experiment

Under the optimal design of uniform design and quadratic universal rotation combination, the optimal doping concentration of phosphor is obtained, and the integral area is obtained [2]. First of all, the theoretical value of the maximum red up-conversion luminescence intensity was 43750 with $1.00\%Ho^{3+}$ and $22.89\%Yb^{3+}$. $NaGd(MoO_4)_2$:Ho^{3+}/Yb^{3+} up-conversion phosphors were synthesized according to the optimal concentration obtained, and their up-conversion emission spectra were measured. The results show that the red up-conversion luminescence integral area of the optimal sample is very close to the theoretical value of 43750.

3.2. Characterization of crystal structure of optimal samples

Figure 2 corresponds to the X-ray diffraction (XRD) plot of the optimal sample concentration for $NaGd(MoO_4)_2$ in Ho^{3+}/Yb^{3+}. The standard card

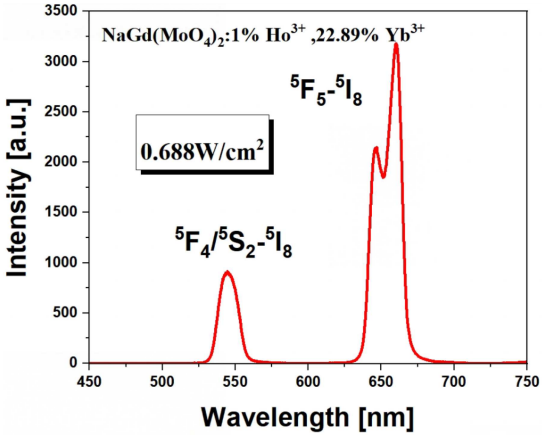

Fig. 1. Up-conversion luminescence emission spectra of the best sample excited by a 980 nm infrared laser.

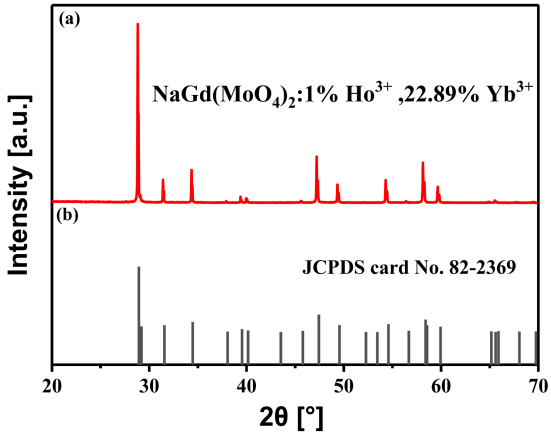

Fig. 2. XRD pattern of the best sample and JCPDS card No. 82-2369 pattern of the standard card.

JCPDS card No. 82-2369 for powder diffraction of $NaGd(MoO_4)_2$ is given in Fig. 2. By contrast, the XRD pattern in Fig. 2 is consistent with the diffraction peak position of the standard card, confirming that the synthesized $NaGd(MoO_4)_2$:Ho^{3+}/Yb^{3+} powder sample is pure phase. Because the ion radii of Gd^{3+}/Ho^{3+}/Yb^{3+} are close to each other, there is no shift in the diffraction peak due to the change of the crystal structure of the co-doped $NaGd(MoO_4)_2$.

3.3. Up-conversion luminescence mechanism for optimal samples

In order to further study the luminescence mechanism of the best sample up-conversion, the red luminescence of the sample is excited and integrated into a 980 nm laser with different working currents. In addition, to avoid the thermal effect of the laser on the sample due to too high excitation power density, the working current of the laser should be kept at a low level, which can reduce the error of the

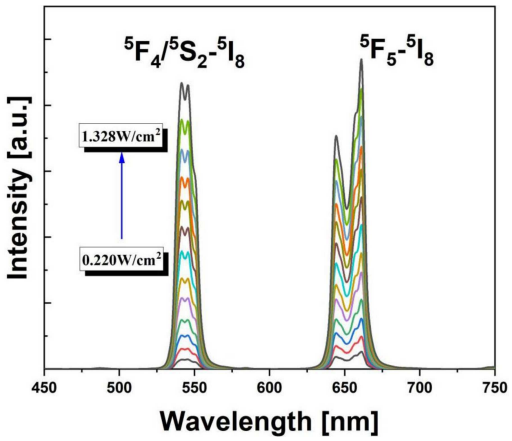

Fig. 3. Up-conversion luminescence emission spectra of an optimal sample excited by a 980 nm infrared laser at different pumping currents.

laser. In order to determine the up-conversion luminescence mechanism of the optimal sample, the dependence of the green and red up-conversion luminescence intensity on the working current of the laser was analyzed. The up-conversion luminescence intensity (I) is related to the working current (i) of the laser as follows [17–19]

$$I = b\left(i - i_0\right)^n. \tag{1}$$

In (1), n is the number of photons required for up-conversion luminescence, b is a constant, and i_0 is the threshold current of the laser. Based on the experimental data of blue up-conversion luminescence intensity of the optimal sample excited by different laser working currents, n values can be obtained by non-linear fitting, and the number of photons required for green and red up-conversion luminescence can be determined. The up-conversion luminescence intensity of $NaGd(MoO_4)_2$:1.00%Ho^{3+} and 22.89%Yb^{3+} was measured at different pump power, as shown in Fig. 3.

As the power increases, the intensity of light emission increases. Logarithmic emission peak intensities corresponding to different pump powers are obtained, and then two straight lines are obtained by linear fitting with the logarithm of pump power, as shown in Fig. 4. The values of n of green emission at 550 nm and red emission at 650 nm are 1.32 and 1.50, respectively. Due to the saturation effect, when the absorption pump power increases, the up-conversion luminescence intensity no longer increases linearly, but gradually tends to saturation. This phenomenon is especially evident in two-photon processes, where two photons are absorbed simultaneously to excite an electron transition. Since the probability of the two-photon process is proportional to the square of the absorbed power, the up-conversion luminescence intensity increases nearly two-fold as the absorbed power increases. So we know that the emission at both of these locations is a two-photon process [20].

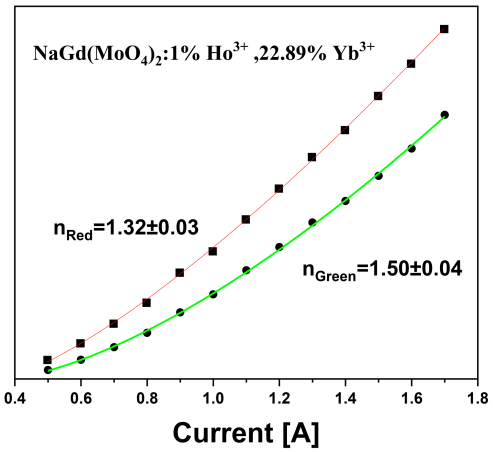

Fig. 4. Dependence diagram of the sample of $NaGa(MoO_2)_4$:1.00%Ho^{3+},22.89%Yb^{3+} with different power supply current and output intensity (980 nm laser).

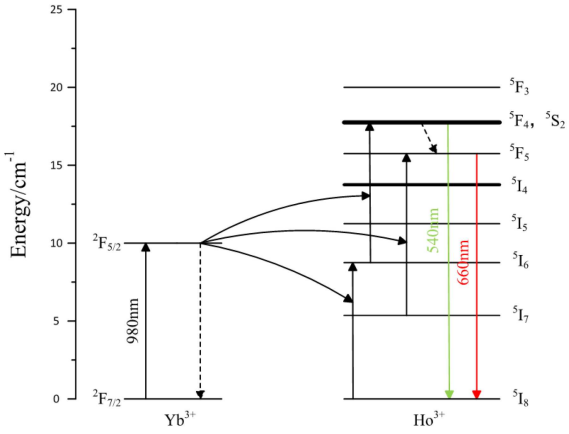

Fig. 5. Diagram of up-conversion luminescence mechanism of Yb^{3+} and Ho^{3+} excited by 980 nm infrared laser.

Figure 5 shows the energy levels of Ho^{3+} and Yb^{3+}. Under the excitation of light at 980 nm wavelength, Yb^{3+} is excited from ground state $^2F_{7/2}$ to excitation state $^5F_{5/2}$. In this process, photons are released to make Ho^{3+} excite from $^5I_8$ to $^5I_6$, and from $^5I_6$ to $^5F_4/^5S_2$, and finally, green light with the main emission position at 550 nm is generated during the process of returning to ground state $^5I_8$. The red light emission at 650 nm is mainly due to the non-radiative relaxation of the electrons at $^5F_4/5F_2$ to $^5F_5$ and then back to the ground state level of $^5I_8$ [21–24].

3.4. Effect of red up-conversion luminescence on temperature

In order to study the temperature quenching behavior of the best sample, the temperature change of the sample was measured by up-conversion emission spectroscopy under 0.688 W/cm^2 laser. It is important to note that each up-conversion emission spectrum measurement is performed under the transient excitation of the laser to avoid the temperature generated by the laser emission which can affect the results.

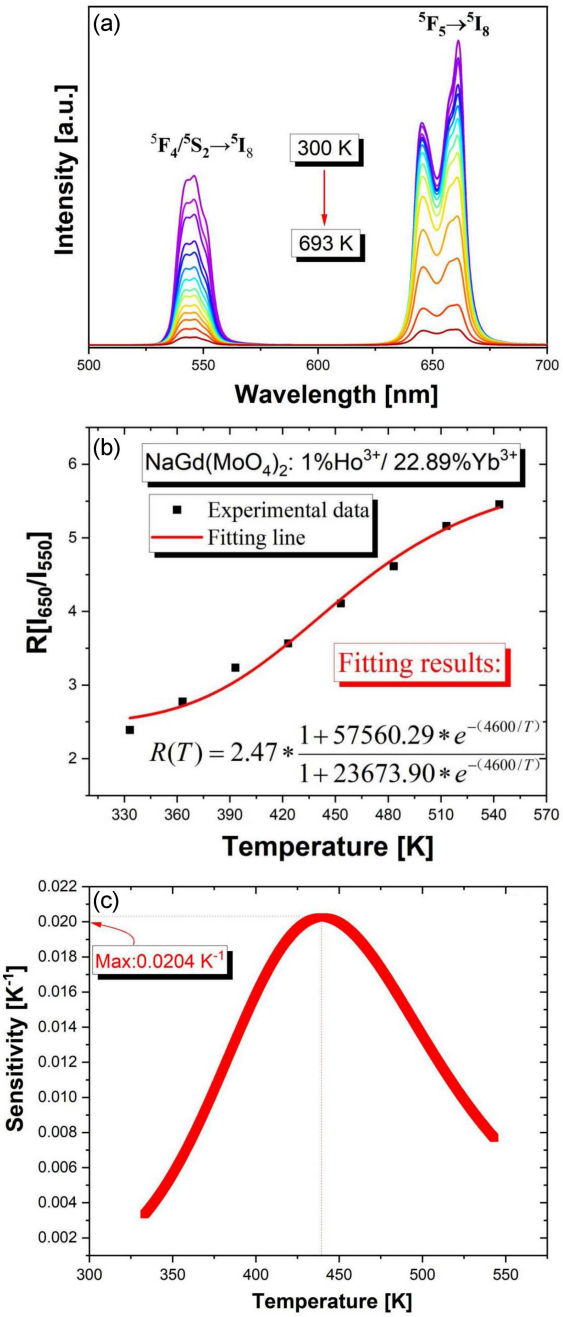

Fig. 6. (a) $NaGd(MoO_4)_2$:(1%Ho^{3+},22.89%Yb^{3+}) emission spectra with temperature; (b) FIR and temperature change and response fitting; (c) relative sensitivity of non-thermally coupled energy levels in relation to temperature.

The emission levels $^5S_2$ and $^5F_5$ of Ho^{3+} belong to a pair of non-thermally coupled levels, and the fluorescence intensity ratio (FIR) between them is usually related to the temperature state of

TABLE I

Temperature sensing properties of up-conversion materials.

Sample	Energy level	Temperature [K]	S_r [K^{-1}]	Ref.
$LiTeO_2$	$^5F_4, ^5S_2 \rightarrow {}^5I_8$	260–400	0.0063	[25]
$NaGdF_4$	$^5F_4, ^5S_2 \rightarrow {}^5I_8$	303–523	0.0051	[26]
$ZnWO_4$	$^5F_4, ^5S_2 \rightarrow {}^5I_8, {}^5I_7$	83–503	0.097	[27]
Y_2O_3	$^5F_4, ^5S_2 \rightarrow {}^5I_8, {}^5I_7$	10–300	0.0067	[28]
$Ba_{0.7}Sr_{0.3}TiO_3$	$^5F_4, ^5S_2 \rightarrow {}^5I_8, {}^5I_7$	80–373	0.02	[29]
$Ba_9Y_2Si_6O_{24}$	$^5F_4, ^5S_2 \rightarrow {}^5F_5$	293–553	0.058	[30]
$NaLaMgWO_6$	$^5F_4, ^5S_2 \rightarrow {}^5F_5$	293–553	0.0089	[31]
$NaGd(MoO_4)_2$	$^5F_5, ^5S_2 \rightarrow {}^5I_8$	300–693	0.0204	this work

the sample. Therefore, the relationship between them can be used to explore their temperature sensing performance. At 980 nm excitation, the up-conversion emission spectrum was measured in the temperature range from 300 to 693 K (Fig. 6a). In the spectrum range of 500–700 nm, it can be clearly seen that the intensity of the emission peak decreases as the temperature increases, indicating that the two non-thermally coupled levels show a certain temperature dependence. Through calculation, it is found that the energy level interval between $^5S_2$ and $^5F_5$ is about 3200 cm^{-1}, which is larger than the maximum distance of 2000 cm^{-1}. Therefore, the FIR temperature sensing of non-thermally coupled levels can be realized by using the FIR law of the up-conversion green and red fluorescence bands of $NaGd(MoO_4)_2$:Ho^{3+}/Yb^{3+} phosphor samples as the temperature changes. Its polynomial formula is as follows

$$\mathrm{FIR} = \frac{I_{540}}{I_{660}} = A + B\,T + C\,T^2 + D\,T^3. \qquad (2)$$

In (2), A, B, C, and D are all constants. The experimental FIR (I_{540}/I_{660}) as a function of temperature can be fitted by (2). The fitting result of FIR is shown in Fig. 6c.

In addition, sensitivity is an important parameter to measure the sensing performance, and the relative sensitivity can be calculated by

$$S_r = \frac{\mathrm{d}\,\mathrm{FIR}}{\mathrm{d}T} = B + 2C\,T + 3D\,T^2. \qquad (3)$$

Figure 6b shows the corresponding function of S_r and the excitation temperature of the 980 nm laser in accordance with the above formula (3). The results in Fig. 6 show that the maximum value of S_r can reach 0.0204 K^{-1} when the sample temperature is 440 K at 980 nm excitation. Also, the temperature sensing performance of Ho^{3+} and Yb^{3+} doped with other substrates has been summarized and is shown in Table I [25–31]. It can be found that the sensitivity of $NaGd(MoO_4)_2$:Ho^{3+}/Yb^{3+} phosphor is higher than most of the materials in the table, which proves that $NaGd(MoO_4)_2$ matrix has a certain application prospect in temperature sensing.

4. Conclusions

Uniform design and quadratic universal rotation design experimental optimization methods were applied, and the optimal concentrations of green luminescence in $NaGd(MoO_4)_2$:(Ho^{3+},Yb^{3+}) fluorescent powder were calculated using a genetic algorithm to be 1% and 22.89%, respectively. Samples were prepared by high-temperature solid-phase method and analyzed by XRD diffractometer as pure phase. The up-conversion emission spectra of $NaGd(MoO_4)_2$:(Ho^{3+},Yb^{3+}) phosphors under 980 nm excitation show two intense bands corresponding to $^5F_4/^5S_2 \rightarrow {}^5I_8$ and $^5F_5 \rightarrow {}^5I_8$ transitions of Ho^{3+} ions. They are in the range of green and red emissions, respectively. Based on the energy level diagrams of Yb^{3+} and Ho^{3+}, as well as the results of power dependence of up-conversion emission intensities, possible excitation pathways for different bands are deduced. The green and red up-conversion emissions of $NaGd(MoO_4)_2$:(Ho^{3+},Yb^{3+}) phosphors originate from the two-photon process. Based on FIR technology, $^5F_4$ and $^5S_2$ are used for temperature measurement. The maximum relative sensitivity is 0.0204 K^{-1} at 440 K, indicating that $NaGd(MoO_4)_2$:(1%Ho^{3+},22.89%Yb^{3+}) has great potential in temperature sensing applications.

Acknowledgments

This work is supported by Funds supported by the National Natural Science Foundation of China (approval number: 52201065).

References

[1] F. Verone, R. Naccache, A.J. Fuente, F. Sanz-Rodriguez, A. Blazquez-Castro, E.M. Rodriguez, D. Jaque, J. García Solé, *ACS Nano.* **2**, 495 (2010).

[2] C. S. Lim, *Trans. Electr. Electron. Mater.* **18**, 1229 (2007).

[3] H.J. Liang, G.Y. Chen, H.C. Liu, Z.G. Zhang, *J. Lumin.* **129**, 197 (2009).

[4] Z.Q. Zheng, X.Y. Li, J. Liu, Z.H. Feng, B.Z. Li, J.W. Yang, K.W. Li, *Physica B Condens. Matter* **403**, 44 (2008).

[5] M.M Li, X. Zhou, Y. Zhang, F. Jiang, S. Sha, S.Q. Xu, S. Li, *Ceram. Int* **46**, 25399 (2020).

[6] V. Ntziachristos, J. Ripoll, L.V. Wang, R. Weissleder, *Nat. Biotechnol.* **23**, 313 (2005).

[7] M. Grzelczak, J. Vermant, E.M. Furst, L.M. Liz-Marzán, *ACS Nano* **4**, 3591 (2010).

[8] K. Maheshvaran, S. Arunkumar, V. Sudarsan, V. Natarajan, K. Marimuthu, *J. Alloys Compd.* **561**, 142 (2013).

[9] X.J. Wang, M.K. Lei, T. Yang, B.S. Cao, *Opt. Mater.* **26**, 253 (2004).

[10] Z. Meng, K. Nagamatsu, M. Higashihata, Y. Nakata, T. Okada, N. Nishimura, T. Teshima, S. Buddhudu, *J. Lumin.* **106**, 187 (2004).

[11] I. Brigger, C. Dubernet, P. Couvreur, *Adv. Drug Deliv. Rev.* **54**, 631 (2002).

[12] S.K. Maurya, S.P. Tiwari, A. Kumar, K. Kumar, *J. Rare Earths* **36**, 903 (2018).

[13] W.H. Fonge, C.W. Struck, *J. Chem. Phys.* **52**, 6364 (1970).

[14] V.K. Rai, D.K. Rai, S.B. Rai, *Sens. Actuator A Phys.* **128**, 14 (2006).

[15] H. Kuhn, M. Fechner, A. Kahn, H. Scheife, G. Huber, *Opt. Mater.* **31**, 1636 (2009).

[16] M.D. Chambers, P.A. Rousseve, D.R. Clarke, *Surf. Coat. Technol.* **203**, 461 (2008).

[17] N.J. Durr, T. Larson, D.K. Smith, B.A. Korgel, K. Sokolov, A. Ben-Yakar, *Nano Lett.* **7**, 941 (2007).

[18] K. Sakthikumar, S.R. Ede, S. Mishra, S. Kundu, *Dalton Trans.* **45**, 8897 (2016).

[19] B. Han, Y.Z. Dai, J. Zhang, X.Y. Wang, W.H. Shi, *J. Lumin.* **196**, 275 (2018).

[20] M. Pollnau, D.R. Gamelin, S.R. Luthi, H.U. Gödel, M.P. Hehlen, *Phys. Rev. B* **61**, 3337 (2000).

[21] T. Zako, H. Nagata, N. Terada, A. Utsumi, M. Sakono, M. Yohda, H. Ueda, K. Soga, M. Maeda, *Biochem. Biophys. Res. Commun.* **381**, 54 (2009).

[22] A. Lukowiak, R.J. Wiglusz, R. Pazak, K. Lemanski, W. Strek, *J. Rare Earths* **27**, 564 (2009).

[23] K.T. Fang, P. Winker, D.K.J. Lin, Y. Zhang, *Technometrics* **12**, 237 (2000).

[24] Y.Z. Liang, K.T. Fang, Q.S. Xu, *Chemom. Intell. Lab. Syst.* **58**, 43 (2001).

[25] A.K. Singh, S.B. Rai, *Appl. Phys. B* **86**, 661 (2007).

[26] E.W. Barrera, Q. Madueño, F.J. Novegil, A. Speghini, M. Bettinelli, *Opt. Mater.* **84**, 354 (2018).

[27] X.N. Chai, J. Li, X.S. Wang, Y.X. Li, X. Yao, *RSC Adv.* **7**, 40046 (2017).

[28] V. Lojpur, M. Nikolic, L. Mancic, O. Milosevic, M.D. Dramicanin, *Ceram. Int.* **39**, 1129 (2013).

[29] Q.H. Zuo, L.H. Luo, Y.J. Yao, *J. Electron. Mater.* **45**, 970 (2016).

[30] J. Zhang, X.W. Li, G.B. Chen, *Mater. Chem. Phys.* **206**, 40 (2018).

[31] J. Zhang, C. Jin, *J. Alloys Compd.* **783**, 84 (2019).